

## EFFECTS OF THE SYNTHESIS METHODS ON THE CATALYTIC ACTIVITY OF PLATINUM AND OSMIUM SUPPORTED ON TITANIA FOR CARBON MONOXIDE OXIDATION

CARLOS H. DELIZ, SANTANDER NIETO

School of Natural Science and Technology, Universidad del Turabo, PO Box 3030, Gurabo, Puerto Rico

(Received 19 Sep, 2019; accepted 01 November, 2019)

**Key words:** Carbon monoxide, X-ray diffraction, Combustion, Global warming

### ABSTRACT

---

---

Platinum and Osmium supported on Titania (Pt/TiO<sub>2</sub>, Os/TiO<sub>2</sub>) catalysts materials were synthesized by solid by solid (SSI), sol-gel (SGI), and incipient wetness impregnation (IWI) techniques. The catalysts were characterized by X-ray diffraction (XRD), SEM, Raman spectroscopy, surface area analysis (BET), and Fourier transforms infrared spectroscopy. *Ex-situ* structural studies by X-ray diffraction and Raman scattering showed that the anatase phase is maintained throughout the 10% of Pt or Os on Titania phase. The experimental demonstrated that supported platinum and osmium are active catalysts at moderate temperature for the complete oxidation of CO to CO<sub>2</sub>; The SSI method gave the most active catalysts for both Pt and Os. Pt catalysts prepared by SSI were active at temperature below 100°C and showed a much greater activity than Osmium catalysts.

---

---

### INTRODUCTION

Carbon monoxides contribute to several environmental hazards to humans, including respiratory illness, global warming, and acid rain. Removal of carbon monoxide from the atmosphere is of vital importance. A viable route for this air removal is through oxidation to CO<sub>2</sub>. For the removal of CO at moderate temperature, it is necessary to catalyze oxidation reaction (Bratan et al., 2014)

There are numerous applications for which a catalyst capable of oxidizing carbon monoxide to carbon dioxide at low temperatures is desirable (Acres and Swart, 2013). Carbon monoxide can form as a result of incomplete combustion of carbon containing materials. For automotive applications, the majority of all emissions (80-90%) are released during the "cold-start" period and materials that have high activity at lower temperatures could help to alleviate pollution from this route (Avgouropoulos et al., 2008). Studies showed that an increase in the ratio of CO to O<sub>2</sub> led to higher O<sub>2</sub> selectivity to CO<sub>2</sub> and lower conversion of CO for a given temperature (Chupin et al., 2006). At a given temperature, the

presence of CO<sub>2</sub> or H<sub>2</sub>O led to an inhibition of the CO oxidation reaction and a decrease in the CO conversion, as compared to the reactions in which CO<sub>2</sub> or H<sub>2</sub>O (Büchel et al., 2009). Stability studies showed that operating the catalyst in its oxide form was fairly stable while operating around 100°C, but operation at higher temperatures (175- 250°C) could lead to a loss of activity, likely caused by the partial reduction of catalytic oxide (Perez et al., 2005). At higher temperatures, the reduction of catalytic oxide also led to the formation of methane through the CO + 2H<sub>2</sub> methanation reaction. Stability studies like cobalt and other catalyst supported on various metal oxide showed that in the test conditions, for example Co/ZrO<sub>2</sub> had the higher activity for the preferential oxidation of carbon monoxide than cobalt on supported on TiO<sub>2</sub>, SiO<sub>2</sub>, CeO<sub>2</sub>, and Al<sub>2</sub>O<sub>3</sub> (Cant et al., 2011). Some precious metals such as Pt, Pd and Au are well known oxidation catalysts and have received significant attention in emission control catalysis (Chupin et al., 2006).

Catalysis is relevant to many aspects of environmental science, e.g. the catalytic converter in automobiles due high cost and the dynamics of

the ozone hole. Catalytic reactions are preferred in environmentally friendly green chemistry due to the reduced amount of waste generated. Platinum group metals dispersed on high surface area oxide supports are used in commercial catalysts. On the other hand, it was found (Kurzman et al., 2013) that the best metal oxide catalyst support was the  $\text{TiO}_2$  due to the strong metal support interaction, chemical stability and acid base property. Among the  $\text{TiO}_2$  allotropic forms, anatase is the only that meet the requirement material for a good catalyst support for metal heterogeneous catalyst, such as high specific surface area and strong interaction with metal nanoparticles (Palcheva et al., 2013; Nolan 2013). From the literature, it is showed that several noble metals particles (Pt, Au, Pd, etc.) when dispersed on a specific group of reducible metal oxide supports, become active for the low temperature oxidation of CO, even at 200K. (Sheintuch et al., 1989; Gardner et al., 1991; Haruta et al., 1991; Gratian et al., 1997)

One significant drawback with these materials, however, is their high cost. To address this concern, a search for lower cost, alternative materials like has led to the study of transition metal catalysts like metallic osmium black (Qu et al., 2015, Figueroa and Newton, 2014). The Osmium tetra oxide form was excluded as a catalyst because its oxide is toxic. Mechanistic studies for example on CO oxidation in excess  $\text{O}_2$  are carried out and transition metal showed cobalt to be an active metal for the reaction, though carbonate formation could lead to decreased activity at temperatures below 100°C. Other studies have shown strong promotional effects of Co and Fe to Pt/ $\text{Al}_2\text{O}_3$  catalysts, leading to substantial activity (Forzatti et al., 2010; Gates and Guilar, 2008) Studies without Pt, using other transition metal catalyst indicate that are active for CO oxidation (Perez et al., 2005). Data found, that the rate of deactivation could be mitigated or eliminated by operating at elevated temperatures or by increasing the ratio of  $\text{O}_2/\text{CO}$ . On the other hand, it was found that one of the largest limitations of the reaction catalytic is the separation and distribution (Hu et al., 2011, Kazuya and Noritake, 2002, Mori et al., 2004). Many of the real catalytic are made of small size (nanometer). This brings as a result the uncertainly and not uniform materials involved, the preparation methods, and surfaces conditions (Kazuya and Noritaka, 2002).

For practical applications of a catalyst, it is of the utmost importance that these work at relatively low temperatures. Existing synthesis techniques normally require high temperatures to crystallize the amorphous material to the desired phase, bringing

in large particles in size and typically non-porous materials. Synthesis methods at low temperatures have recently achieved crystalline titania with a high degree of control in the formed polymorph and in their porosity.

The preparation of any catalysts involves a series of complex processes, which many of them are not fully understood yet. Consequently, small changes in the preparation can be a critical factor in the final properties of the catalyst. One of the important requirements in any method of preparation is the high surface area, because the reactants must have accessibility to a maximum number of active sites. Some of these parameters are dependent on the method of preparation. A critical factor important, it is the optimal conditions for catalyst supported titanium preparation, which one should be optimized, in terms of pretreatment and activation (Lin et al., 1993; Gallardo et al., 1995).

Therefore, parameters like sintering (Yan et al., 2005), alloy formation (Park and Seol, 2007), encapsulation, and inter diffusion (Ren et al., 2007), will produced morphological changes originated from titania support interaction [Yan et al., 2005; Park and Seo, 2007; Ren et al., 2007) For a particular metal heterogeneous catalyst.

In this paper, our goal was to investigate the effect of the oxidation of carbon monoxide to carbon dioxide on the synthesis parameters and also study the effect on CO oxidation activity of Platinum and Osmium supported on titania catalysts materials prepared by solid by solid (SSI), sol-gel (SGI), and incipient wetness impregnation (IWI) techniques. These methods proposed, permit to get good catalyst at relatively low temperature and also allow stoichiometry to be controlled.

## MATERIALS AND METHODS

### Catalyst Preparation

The catalysts were synthesized by the incipient wetness impregnation (IWI), sol-gel (SGI) synthesis and solid by solid impregnation technique (SSI). The IW technique involves the addition of metal (osmium or platinum) solution 10% (0.5 grams) in water (50 mL) mixed with 5 grams of porous catalyst support such as  $\text{TiO}_2$ . The solution was added drop wise in excess (water) to cover all pore volume of the support. Catalyst was placed in a drying oven at 110°C to evaporate the water. Catalyst was calcination with ramp rate of 10°C/hour to 300°C.

Sol-gel synthesis employs a controlled hydrolysis reaction of a metal alkoxide precursor with an

aqueous solution containing the catalyst's active metal. The solution containing the active metal with water, 5 mL was added to the stirred mixture the alkoxide precursor at a rate of 0.2 mL/min using a syringe pump. Note: Additional 5 mL of water to increase the rate of the hydrolysis at 2:1 ratio. 0.500 g metal /5 mL water = 0.10 g/ mL. Density Titanium (IV) isopropoxide 0.960 g/mL. 5.20 mL (0.960 g/mL)=5 g Titanium (IV) isopropoxide.  $(0.10/0.960) \times 100\% = 10\%$  Ti  $\{OCH(CH_3)_2\}_4 + 2 H_2O \rightarrow TiO_2 + 4 (CH_3)_2CHOH$ .

The impregnation solid by solid technique involves the addition of metal (osmium or platinum) 10% mixed with porous catalyst support,  $TiO_2$ . 10%=0.5 grams metal/5 grams  $TiO_2$ . The final impregnation step, the catalysts were calcined for at least 3 hours at 300°C. The dried powder was then mixed and crushed using a mortar and mechanic catalytic mixer (Qu et al., 2015; Figueroa and Newton, 2014).

All the incipient wetness impregnated catalyst in these studies used distilled water as the solvent to dissolve the  $TiO_2$  support (Titanium (IV) Acros lot: 277370010) with the active component, metallic osmium black (99.9% Acros) was added/impregnated onto the support. The solution was added drop wise so that then total volume of the solution added to the support. The same procedure was applied to Pt/ $TiO_2$  (metallic platinum black 98.0% Acros) support on (Titanium (IV) Acros). After the impregnation, the catalyst was placed in a drying oven at 110°C to evaporate the solvent, leaving the metal on the catalyst support. In some cases, multiple impregnations were used to help reduce possible variations between different particles which could have not been well impregnated.

Following the final impregnation step, the catalysts were calcined in air using a ramp rate of 10°C/hour to 300°C then held at the final calcination temperature for at least 3 hours. Sol-gel synthesis employs a controlled hydrolysis reaction of a metal alkoxide precursor (Titanium (IV) isopropoxide) Acros lot: A0342321 with an aqueous solution containing the catalyst's active metal. The synthesis of sol-gel catalyst was based on 5 grams of catalyst (Derrouchide and Bianchi, 2006).

The alkoxide precursor was mixed in a beaker with 50 mL of isopropanol, using a magnetic stir bar. In a separate container, the active metal was dissolved in an aqueous solution and placed in a syringe. To increase the rate of the hydrolysis reaction, the amount of water that was used during the synthesis was greater than the necessary stoichiometric quantity, and a 2:1 ratio of water to metal alkoxide

were used. The aqueous solution containing the active metal was added to the stirred mixture of isopropanol and the alkoxide precursor at a rate of 0.2 mL/min using a syringe pump. After the aqueous solution was completed added to the beaker, the gel was left to dry overnight (Gavinchua et al., 2014). The dried powder was then mixed/crushed using a mortar and pestle and the powder was subsequently calcined in the same manner that was used from the catalyst prepared by incipient wetness impregnation.

### Measurements of Catalytic Performance for CO Oxidation

Laboratory-microscale reaction experiments were performed on the reactor system depicted in Fig. 1. The system was equipped with flow controller (ADM1000 Intelligent Flow meter JW) and allowed a wide range of gas velocities to be introduced to the reactor. The reaction temperature was controlled by Lindberg Blue M Thermo Scientific tubular oven and temperature K-type thermocouple linked model Fluke, designed to run at temperatures up to maximum 700°C. The reactor was constructed from ¼ external diameter stainless steel and copper tubing. The catalyst samples were held in cylindrical reactor of 50 mm high × 4.6 mm diameter (Kohyama et al., 2015; Haruta et al., 1993; NIST). Equilibrium composition of CO oxidation was a highly exothermic reaction and was quite temperature sensitive, so the thermocouple was positioned so it touched the downstream end of the catalyst bed, this ensured an accurate temperature reading that accounts for the heat produced in the reaction (Ingelsten et al., 2005). Screening experiments were compared catalysts based on equal weights as platinum black support on titanium dioxide. The temperature range for testing covered the range of 25°C to 200°C. A variety of analytical equipment was used to monitor the feed and product gas stream compositions. A Bacharach Fyrite Tech Infrared Analyzer provided simultaneous and continuous monitoring of CO and  $CO_2$  concentrations (Lindholm et al., 2008; Burrows et al., 2007). In addition, simultaneous measurement with GC 5890 HP gas chromatograph equipped with a thermal conductivity detector (TCD) and 5A molecular sieve column as well as phenomenex column. The catalyst was pre-treated in helium flow at 200°C for a period of 30 min to remove any volatile contaminant and adsorbed gases.

### Material Characterization

The powder X-ray diffraction tests were carried out using a Bruker D8 Advance system in a Bragg-Brentano vertical goniometer configuration. The

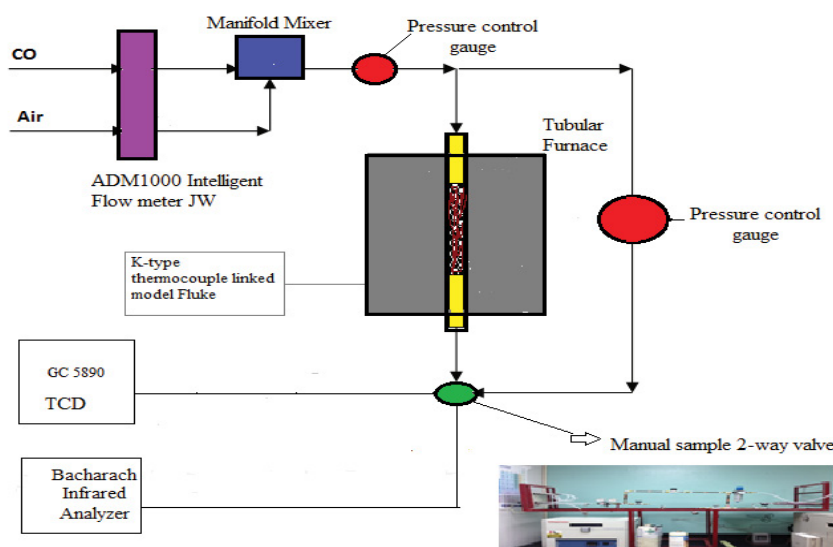


Fig 1. The experimental oxidation setup.

phase formation behavior of the calcined powder was characterized by XRD using Cu-K radiation in the  $2\theta$  ranges of  $15^\circ - 70^\circ$ . Selected diffraction peaks were slow scanned at a scanning speed of 0.30–1.0 min. From the recorded XRD pattern, the accurate peak position ( $2\theta$ ) as well as the full-width at half maxima (FWHM) ( $\beta$ ) of each slow scanned diffraction peaks was estimated by fitting the diffraction peak with Pearson VII amplitude function using a commercial peak fit software. These values were used to calculate the crystallite size and lattice strain of the synthesized powder using Williamson Hall equation (Williamson and Hall, 1953).

The SEM study was carried out with a JEOL JSM 6360 microscope in secondary electron mode at an accelerating voltage of 20 kV to image the surface of the anatase powder. The sample grains were adhered to the sample holder with an adhesive tape. The surface morphology was revealed from SEM images and the grain size was calculated with the help of the software provided by the microscope.

Raman measurements were performed using a Raman Renishaw spectrophotometer consisting a double monochromator coupled to a third monochromator/spectrograph with 1800 grooves/mm grating. The 785 nm radiation of an  $\text{Ar}^+$  laser was focused in a less than  $2 \mu\text{m}$  diameter circle area by using Raman micro-probe with an 80x objective. The same microscope was used to collect the signal in back scattering geometry and to focus it at the entrance of the monochromator. The scattered light dispersed by the spectrophotometer was detected by a charge coupled device detection system. The infrared Fourier transform spectra were gathered using a Nicole Protégé Model 4700 Thermo Electron

spectrometer, data were collected at a resolution of  $4 \text{ cm}^{-1}$  employing 100 scans per sample at room temperature under  $\text{N}_2$  flow (Praxair 99%) at a rate of 50 cc/min.

Surface area analysis was performed over supported metallic osmium catalysts 10% Os/ $\text{TiO}_2$  using BET method with a Micromeritics TriStar II 3020 instrument.  $\text{N}_2$  was selected as the adsorbent, and analysis was performed at liquid nitrogen temperature (77 K). The samples were degassed before surface area measurement (Xianyong et al., 2014; Wonyong et al., 2014; Gas Adsorption Theory).

## RESULTS AND DISCUSSION

### X-ray diffraction

An x-ray diffraction pattern was used for identification of the crystal phase and estimation of the crystallite size of each phase. Fig. 2 and 3 shows the XRD patterns of Titanium and metal supported  $\text{TiO}_2$  catalysts. In all samples we can see the presence of the anatase phase. The peaks at  $2\theta=25.3$  (101),  $39.8^\circ$  (112),  $48^\circ$  (200) and  $53.9^\circ$  (211) in the spectra of all samples are easily identified as the crystal of anatase form [PDF# 84 - 1286]. The patterns did not show any peaks for loaded metal oxides, indicating that these metal oxides were well dispersed in all cases. The crystallinity of the polycrystalline metal/ $\text{TiO}_2$  was determined from the peak intensities and peak widths of the diffraction lines. To obtain accurate peak position ( $2\theta$ ) as well as FWHM values ( $\beta$ ) these peaks were fitted to Pearson VII amplitude function using a commercial Peakfit-4 program. After correcting the instrumental broadening (Cullity 1978), the remaining line broadening ( $\beta$ ) is believed to be due to the crystallite size ( $\beta_{\text{cryst}}$ ) and retained

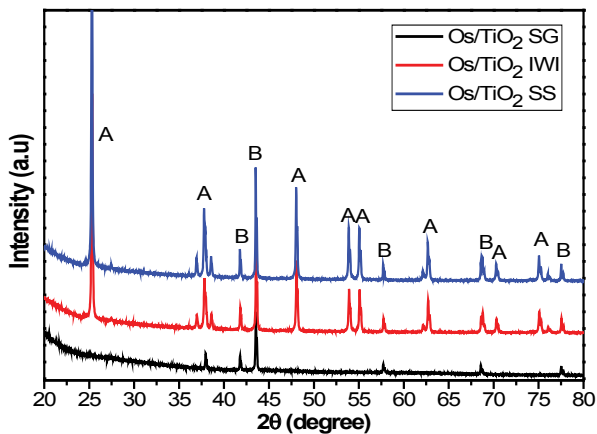


Fig 2. X-ray diffractogram of Os supported TiO<sub>2</sub> catalysts synthesized by a) SGI, b) IWI, and c) SSI route

strain ( $\beta$  strain) broadening (Williamson and Hall, 1953). From Scherrer's equation (Cullity 1978).

$$t = \frac{K\lambda_{X-RAY}}{\beta \cos \theta}$$

Where  $t$  is the crystallite size,  $\lambda_{X-ray} = 0.15418$  nm,  $K$  is usually taken as 0.89,  $\theta$  is the Bragg's diffraction angle, and  $\beta$  is the line width at half-maximum height, after subtraction of equipment broadening. The crystallite parameter of the obtained powder is shown in Table 1.

### SEM Study

Morphology of the powder was observed with scanning electron microscope and Fig. 4 shows the SEM pictures of Os/TiO<sub>2</sub> and Pt/TiO<sub>2</sub> powder prepared by different synthesis methods. We can see a very fine particle size of the synthesized catalysts, compose of approximately 10-50 nm particles which are aggregated together to form bigger assemblies. It is believed that the interparticle mesoporous are responsible for the good catalytic activity of these catalysts. These inter particle mesopores are an important contribution to the measured high surface area 102.7 m<sup>2</sup>/g. Further, the stoichiometry of the prepared composition has been verified using EDAX analysis (not shown here). The stoichiometry of metal (Os and Pt) was examined. The results of the prepared composition atomic concentration were reported in the Table 1.

With the previously reported particle size data it is possible to estimate the catalyst surface area by assuming all the particles to have same spherical shape and size (Jiaqiao and Baiyun, 2001) with the help of the following relation

$$S = 6/\delta\rho$$

Where the  $\delta$  is the particle size and  $\rho$  is the material

density. Since  $\delta = 15$  nm and  $\rho = 3.895$  gcm<sup>-3</sup> is the anatase density, the specific surface,  $S$ , is 102.7 m<sup>2</sup>g<sup>-1</sup>. The value previously calculated is in good agreement with the parameter measured with the help of the

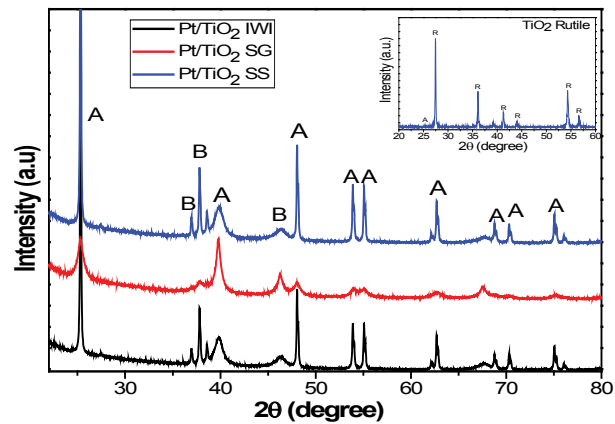


Fig 3. X-ray diffractogram of Pt supported TiO<sub>2</sub> catalysts synthesized by a) IWI, b) SGI, and c) SSI route.

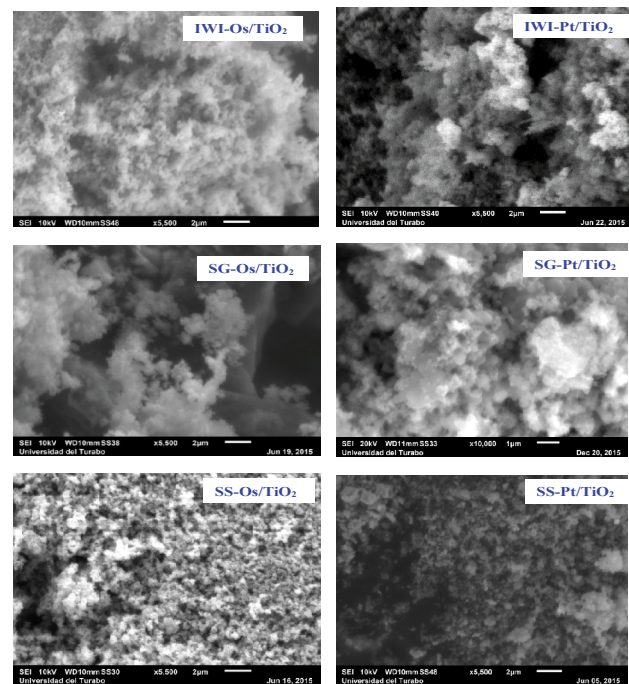


Fig 4. SEM micrographs of metal/TiO<sub>2</sub> (Os/TiO<sub>2</sub> and Pt/TiO<sub>2</sub>) powders prepared by (a-b) Impregnation route, (c-d) Sol Gel process, and (e-f) Solid State Solution.

Table 1. Summary of the stoichiometry of the catalysts synthesized.

Catalyst	Synthesis Technique	TiO <sub>2</sub> wt %	Oxygen wt %	Metal wt %
10% Os/TiO <sub>2</sub>	IWI	65.26%	25.93%	8.81%
10% Os/TiO <sub>2</sub>	SGI	53.11%	32.12%	13.77%
10% Os/TiO <sub>2</sub>	SSI	45.52%	42.15%	12.33%
10% Pt/TiO <sub>2</sub>	IWI	54.51%	32.50%	12.99%
10% Pt/TiO <sub>2</sub>	SGI	55.14%	37.18%	7.68%
10% Pt/TiO <sub>2</sub>	SSI	72.10%	18.85%	9.05%

BET method. The performance of the catalyst can be influenced by the sintering conditions. Further studies are required to clarify these issues.

### Raman Spectroscopy

Raman spectra were obtained on powder samples at room temperature prepared by different synthesis methods. In Fig. 5 and 6 is shown the Raman spectra of the catalysts (Os/TiO<sub>2</sub> and Pt/TiO<sub>2</sub>) synthesized for the three methods, the impregnated solid by solid, sol-gel and IWI, respectively. It is well known that the anatase phase has six Raman active modes: a peak with strong signal appears at 144 cm<sup>-1</sup> followed by low intensity peaks located at 197, 399, 513, 519, and 641 cm<sup>-1</sup>. All Raman spectra confirm the anatase phase of this TiO<sub>2</sub> nanopowder (some of them are shown in Fig. 5 and 6). Raman modes can be assigned to the Raman spectra of the anatase single crystal (Ohsaka et al., 1978): ~144 (E<sub>g</sub>), 197 (E<sub>g</sub>), 399 (B<sub>1g</sub>), 513 (A<sub>1g</sub>), 519 (B<sub>1g</sub>) and 639 cm<sup>-1</sup> (E<sub>g</sub>). The broadening of the TiO<sub>2</sub> bands may be attributed to interactions with Os and Pt species and disorder in the oxygen sub-lattice (Hamilton et al., 2014). These results indicate that osmium and platinum were presents in the Os/TiO<sub>2</sub> and Pt/TiO<sub>2</sub> catalyst, respectively (Hao et al., 2009).

The lack of metallic osmium raman bands at lower calcinations temperatures on the TiO<sub>2</sub> supported samples suggests that Os does not form as readily on the surface as compared to the TiO<sub>2</sub> support. This difference in surface Os is likely related to the differences in CO oxidation activity observed over the TiO<sub>2</sub> catalysts. These results indicate that osmium and platinum were presents in the Os/TiO<sub>2</sub> and Pt/TiO<sub>2</sub> catalyst (Hao et al., 2009). The lack of clearly visible vibrational bands from the TiO<sub>2</sub> support in the sample Os/TiO<sub>2</sub> can was explained by the smaller Raman cross-section of anatase tetragonal forms of TiO<sub>2</sub>. The broadening of the TiO<sub>2</sub> bands may be attributed to interactions with Os and Pt species and disorder in the oxygen sub-lattice (Hamilton et al., 2014).

### FT-IR Study

The adsorption spectra of the 10% Os/TiO<sub>2</sub> and 10% Pt/TiO<sub>2</sub> were obtained to examine the types of surface species using a FT-IR Nicole Protégé Model 470. For 10% Os/TiO<sub>2</sub> sol-gel impregnation, the high wave number region in Fig. 6 exhibits bands at 3500 cm<sup>-1</sup> that correspond to terminal, bi-bridged, and tri-bridged OH groups, typical of the OH vibration of physically adsorbed H<sub>2</sub>O (Yasuo et al., 2009; Young and Meijun, 2007). For SGI, IWI and SSI were observed by a combination band at 2900 cm<sup>-1</sup> and the

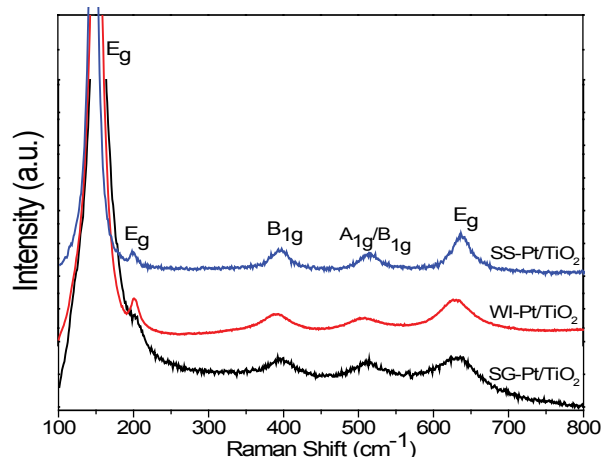


Fig 5. Raman spectra of Pt supported TiO<sub>2</sub> catalysts synthesized by a) SGI, b) IWI, and c) SSI methods.

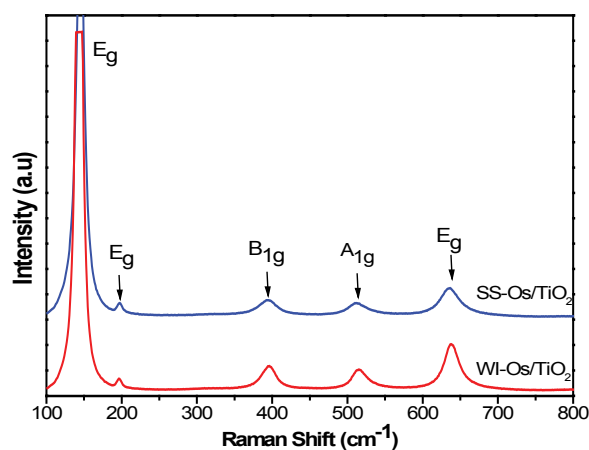


Fig 6. Raman spectra of Os supported TiO<sub>2</sub> catalysts synthesized by a) IWI, and c) SSI methods.

C-H stretch at 2800 cm<sup>-1</sup>. In the low wave number region, Fig. 6 and 7 were observed from the band at 1484 cm<sup>-1</sup> as well as the C-H bending and symmetric C-O stretching modes at 1379 cm<sup>-1</sup> at 1358 cm<sup>-1</sup>, respectively (Hao et al., 2015). Other bands in the 1000-500 cm<sup>-1</sup> have been assigned to ionic carbonate at 1484 cm<sup>-1</sup> which shifts to 1440 cm<sup>-1</sup> and carbonate species at 1300 cm<sup>-1</sup> and 700 cm<sup>-1</sup> (Chen et al., 2010).

### Activation Energy

The Arrhenius plot shown in Fig. 9, and the activation energy for oxidation of CO to CO<sub>2</sub> over 10%Os/TiO<sub>2</sub> and 10% Pt/TiO<sub>2</sub> were calculated Table 2. The Sol-gel technique in both platinum and osmium preparation required less activation energy, so the reactions occur more faster (An et al., 2014; Zhao et al., 2009; An et al., 2011; Hafizovic et al., 2007). The Arrhenius plot was obtained by plotting the logarithm of the rate constant, *k*, versus the inverse temperature, 1/*T* (Perez et al., 2005).  $k=Ae^{-E_a/RT}$  where *k* represents the rate constant, *E<sub>a</sub>* is the activation energy, *R* is the

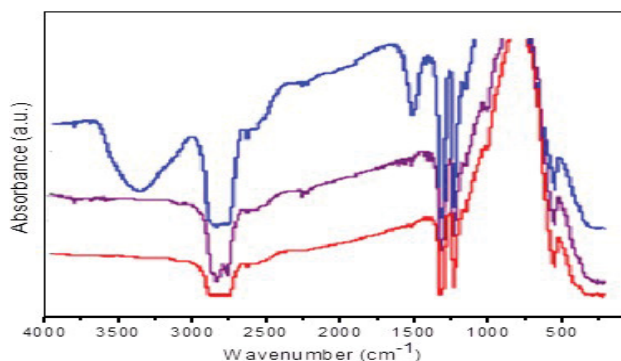


Fig 7. FT-IR spectra of the Os/TiO<sub>2</sub> catalysts synthesized by a) SGI, b) IW, and c) SSI methods.

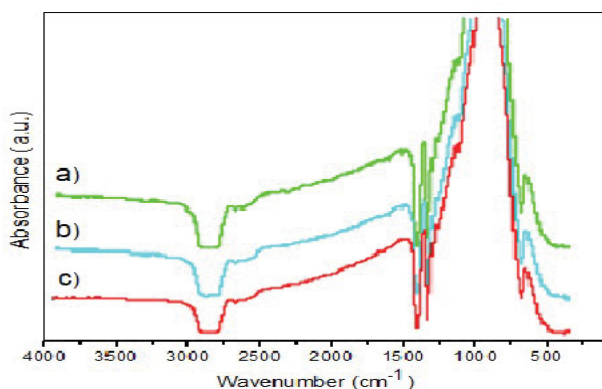


Fig 8. FT-IR spectra of the Pt/TiO<sub>2</sub> catalysts synthesized by a) SGI, b) IW, and c) SSI methods.

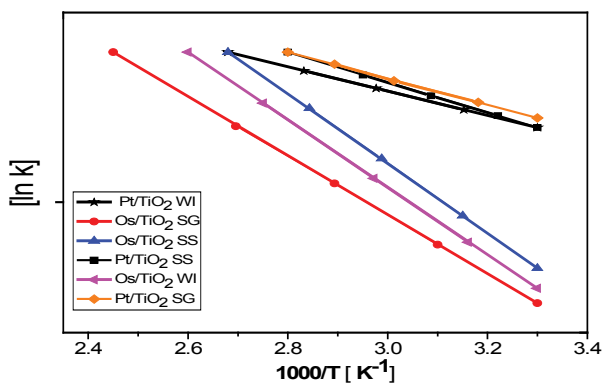


Fig 9. The Arrhenius plot of the Os/TiO<sub>2</sub>, and Pt/TiO<sub>2</sub> catalysts synthesized by a) SGI, b) IW, and c) SSI route.

gas constant (8.3145 J/K) and T is the temperature expressed in Kelvin. A is known as the frequency factor, having units of L/mol.s. We can graphically determine the activation energy by manipulating the Arrhenius equations to put it into the form of a straight line. Taking the natural logarithm of both sides give us;  $\ln k = -E_a/RT + \ln A$ . A slight rearrangement of this equation then gives us a straight-line plot for  $\ln k$  versus  $1/T$ , where the slope is  $-E_a/R$ .  $\ln k$  (rate constant) data were obtained knowing gas flow velocities (45 mL/minutes) and reactor volume. The

value obtained was multiplied by the percentage obtained at the temperature required to complete the entire conversion of CO to CO<sub>2</sub>.

**Catalytic Activity**

The catalytic activity was in terms of % conversion. (X) of CO gas to CO<sub>2</sub> according to the following equation:  $X_{CO} = (\text{ppm CO in} - \text{ppm CO}_2 \text{ out}) / \text{ppm CO in} \times 100$ . Time-on-stream studies at room temperature (25°C) were conducted on the 10% Os/TiO<sub>2</sub> catalyst using feed streams containing 300 ppm CO (Industrial Scientific) in balance with air. Fig. 10 shows the concentrations of CO and CO<sub>2</sub> during the experiment using a feed stream of 45 mL/min. Complete conversion of CO to CO<sub>2</sub> was obtained and no decline in conversion was observed over the course of this experiment. To further study the catalyst's activity, an additional experiment was conducted using 10% Pt/TiO<sub>2</sub> standard catalyst under same conditions. The CO<sub>2</sub> was the only product that was formed (Lonergan et al., 2011). During this experiment, the temperature was increased by temperature increments of 25°C. The higher CO concentration in the experiment required elevated temperatures in order to achieve complete conversion of CO to CO<sub>2</sub>, which was obtained at 80°C in sol-gel and solid by solid impregnation with 10%

Table 2. Summary of the activation energies measured of Pt/TiO<sub>2</sub> and Os/TiO<sub>2</sub> catalyst.

Catalyst	Synthesis method	Activation energy (kJ/mol)
Pt/TiO <sub>2</sub>	SSI	22
	SGI	25
	IWI	57
Os/TiO <sub>2</sub>	SSI	59
	SGI	21
	IWI	50

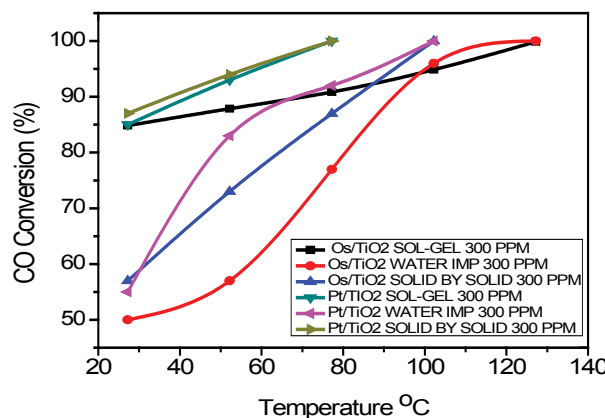


Fig 10. Co oxidation activity over 10% wt Os/TiO<sub>2</sub>, and Pt/TiO<sub>2</sub> catalysts synthesized by a) SGI, b) IW, and c) SSI route.

Pt/TiO<sub>2</sub> like referent standard (Rivallan et al., 2014). The other way with 10% Os/TiO<sub>2</sub> was obtained at 100°C in sol-gel and solid by solid impregnation. The IWI in both case, the completed conversion to 10% Os/TiO<sub>2</sub> about 130°C and 10% Pt/TiO<sub>2</sub> about 100°C. The experiment was run over the course of several days and the catalyst was shown to be stable during the experiment, with no decline in activity at any of their ported temperatures. It can be observed in sol-gel impregnation to both catalysts that the decrease in CO concentration was accompanied by the simultaneous and fast increase in CO<sub>2</sub> concentration (Tsao et al., 2007). However, water impregnation to both catalysts, there appeared to be some inhibition effect, with temperature required for complete CO conversion shifting by about 50°C (Liu et al., 2015; Ning et al., 2015; Lonergan et al., 2011). Water impregnation in Fig. 10 shows that complete conversion of CO was not obtained until about 135°C to 10% Os/TiO<sub>2</sub> and 100°C to 10% Pt/TiO<sub>2</sub>, possibly due to a competitive adsorption effect. Osmium based catalysts have been synthesized and studied both for the low temperature oxidation of CO in low oxygen as well as for the preferential oxidation of CO were found that high activity could be achieved even at room temperature (Kohyama et al., 2015; Haruta et al., 1993; Iizuka et al., 2009]. The reaction studies examined the effect of water, which was found to have an inhibitory effect on CO oxidation.

## CONCLUSION

High increasing demand of catalysts for industrial and environmental applications, it is of prime importance to search for improved supports for a variety of reactions. The high activity of catalyst is also of prime importance, which effectively reduces the amount of expensive catalyst. Considering the increasing cost of noble metal-based catalysts for environmental applications, as well as their limited availability, it is of most importance to develop new catalysts with improved catalytic activity under the conditions of practical relevance. 100% CO to CO<sub>2</sub> conversion was observed in a temperature range 50–140°C using micro scale reactor, on space velocity 3250 h<sup>-1</sup> and initial CO concentrations at 300 ppm. This is of interest for industrial CO control, where the off gas temperature was often low, because of the use of dry scrubber to remove the poisonous gases or for automotive applications, the majority of all emissions (80-90%) are released during the “cold-start” period. For the oxidation catalysts, osmium supported on TiO<sub>2</sub> was shown to have high activity. Sol-gel and solid by solid synthesis techniques were examined, with overall higher activity. Studies

using SEM, XRD, FT-IR, UV, BET and Raman spectroscopy were consistent with this observation and its characterization; however, platinum was more oxidized and faster in TiO<sub>2</sub>. Osmium could be alternative material. Osmium was proposed as a good candidate because it has been shown to be active for CO oxidation and is less expensive than gold and platinum. Concluded that the presence of osmium and the support's ability to promote the formation of CO<sub>2</sub>. The oxidation of CO was complete over most of the temperature range, indicating that the osmium mixed catalyst bed can work to eliminate CO. Tree rings have been used as proxies to establish pollution chronology from vehicular emission into the atmosphere for a period spanning from 1957 to 2018. Tree growth rings have been related to annual rainfall patterns. From this study, high precipitation (wet seasons) has been linked to increased growth of tree rings. No growth of tree rings has also been linked to harsh environmental conditions such as drought (dry seasons).

Pollution trends from vehicular emissions, which contribute to the increase of Zinc, Copper, Lead, Manganese and Cadmium in the atmosphere, have been determined over a period from 1957 to 2018. A worrying trend observed for almost all the heavy metals as the levels of these metals have been increasing exponentially over the past decades. This raises lots of concerns because if this trend is not halted, it can disturb the study area as some heavy metals recorded values which exceed the WHO guidelines on the limits of these metals.

## REFERENCES

- Acres, K., Swart, K. (2013). *Gmelin Handbook of inorganic and Organometallic Chemistry*. (8th edn) 3:32-140.
- An, J., Shade, C. M., Chengelis-Czegan, D. A., Petoud, S., Rosi, N. L. (2011). Zinc-adeninate metal-organic framework for aqueous encapsulation and sensitization of near-infrared and visible emitting lanthanide cations. *J. Am. Chem. Soc.* 133:1220-1223.
- An, Z., He, J., Dai, Y., Yu, C., Li, B., He, J. (2014). Enhanced heterogeneous asymmetric catalysis via the acid-base cooperation between achiral silanols of mesoporous supports and immobilized chiral amines. *J. Catal.* 317:105-113.
- Avgouropoulos, G., Manzoli, M., Boccuzzi, F., Tabakova, T., Papavasiliou, J., Loannides, T., Idakie V. (2008). Catalytic performance and characterization of Au/doped-ceria catalysts for the preferential CO oxidation reaction. *Catal J.* 256: 237-247.

- Bratan, V., Munteanu, C., Hornoiu, C., Papa, F., Ionescu, N. (2014). Study of CO oxidation over TiO<sub>2</sub> anatase by simultaneous kinetic and electrical measurements. *Reac Kinet Mech Cat.* 112: 51-60.
- Büchel R., Strobel R., Krumeich F., A. Baikerb, S.E. (2009). Pratsinis SE. Influence of Pt location on BaCO<sub>3</sub> or Al<sub>2</sub>O<sub>3</sub> during NO<sub>x</sub> storage reduction. *J. Catal.* 261:201-207.
- Burrows, A.K., Kiely, C., Wachs, I. (2007). Molecular/electronic structure-surface acidity relationships of model-supported tungsten oxide catalysts *J. Catal.* 246:370-381.
- Cant, N.W., Chambers, D.C., Liu, I. (2011). The reduction of 15N-14N-O by CO and by H<sub>2</sub> over Rh/SiO<sub>2</sub>: A test of a mechanistic proposal. *J. Catal.* 278:162-166.
- Chen, Z., Yang, Q., Li, H., Li, X. Wang, L., Tsang, S.C. (2010). Cr-MnO<sub>x</sub> mixed-oxide catalysts for selective catalytic reduction of NO<sub>x</sub> with NH<sub>3</sub> at low temperature. *J. Catal.* 276:56-65.
- Chupin, C., Van-Veen, A.C., Konduru, M., Després, J., Mirodatos, C. (2006). Identity and location of active species for NO reduction by CH<sub>4</sub> over Co-ZSM-5. *Catal J.* 241:103-114.
- Cullity, B.D. (1978). *Elements of X-ray diffraction*, Addison-Wesley, New York, USA, 1978, p. 281.
- Derrouiche, S., Bianchi D. (2006). Modifications of the elementary steps involved in the O<sub>2</sub>-oxidation of the adsorbed CO species over Pt/Al<sub>2</sub>O<sub>3</sub> by co-adsorbed NO species. *J. Catal.* 242:172-183.
- Figuroa S., Newton. M., *Catal. J.* (2014). What drives spontaneous oscillations during CO oxidation using O<sub>2</sub> over supported Rh/Al<sub>2</sub>O<sub>3</sub> catalysts? 312:69-77.
- Forzatti, P., Lietti, L., Nova, I., Morandi, S., Prinetto, F., Ghiotti, G. (2010). Reaction pathway of the reduction by CO under dry conditions of NO<sub>x</sub> species stored onto PtBa/Al<sub>2</sub>O<sub>3</sub> Lean NO<sub>x</sub> Trap catalysts *J. Catal.* 274:163-175.
- Gallardo Amores, J. M., Sanchez Escribano, V., Busca, G. (1995). Anatase crystal growth and phase transformation to rutile in high-area TiO<sub>2</sub>, MoO<sub>3</sub>-TiO<sub>2</sub> and other TiO<sub>2</sub>-supported oxide catalytic systems. *Journal of Materials Chemistry.* 5:1245-1249.
- Gardner, S.D., Hoflund, G.B., Schryer, D.R., Upchurch, B.T. (1991). Characterization study of silica-supported platinized tin oxide catalysts used for low-temperature carbon monoxide oxidation: effect of pre-treatment temperature. *J. Phys. Chem.* 95:835-838.
- Gates, B., Guilar. V. (2008). Kinetics of CO oxidation catalyzed by highly dispersed CeO<sub>2</sub>-supported gold *J. Catal.* 260:351-357.
- Gavin Chua, Y.P., Kasun Kalhara Gunasooriya, G.T., Saeys, M., Seebauer E. (2014). Controlling the CO oxidation rate over Pt/TiO<sub>2</sub> catalysts by defect engineering of the TiO<sub>2</sub> support *J. Catal.* 311:306-313.
- Gratian R., Bamwenda, Tsubota, S., Nakamura T., Haruta, M. (1997). The influence of the preparation methods on the catalytic activity of platinum and gold supported on TiO<sub>2</sub> for CO oxidation. *Catalysis Letters* 44:83-87.
- Hafizovic, J., Bjørgen, M., Olsbye, U. Dietzel, P. D. C., Bordiga, S., Prestipino, C., Lamberti, C., Lillerud, K. P. (2007). the inconsistency in adsorption properties and powder XRD Data of MOF-5 is rationalized by framework interpenetration and the presence of organic and inorganic species in the nanocavities *J. Am. Chem. Soc.* 129:3612-3620.
- Hamilton, N., Warringham, R., Silverwood, I., Kapitán, J., Hecht, L., Webb, P., Tooze, R., Wuzong, W., Frost, C., Parker, S., Lennon. D. (2014). The application of inelastic neutron scattering to investigate CO hydrogenation over an iron Fischer-Tropsch synthesis catalyst. *J. Catal.* 314:221-231.
- Hao, Y., Hongjuan, P., Feng, N., Xiaomei, P. (2015). Pt nanoparticles interacting with graphitic nitrogen of N-doped carbon nanotubes: Effect of electronic properties on activity for aerobic oxidation of glycerol and electro-oxidation of CO. *J. Catal.* 325:136-144.
- Hao, Y., Mihaylov, M., Ivanova, E., Hadjiivanov, K., Knözinger, H., Gates. B. CO oxidation catalyzed by gold supported on MgO: Spectroscopic identification of carbonate-like species bonded to gold during catalyst deactivation (2009). *J. Catal.* 261:137-149.
- Haruta, M., Tsubota, S., Kobayashi, T., Kageyama, H., Genet M.J., Delmon, B. (1993). Low-temperature oxidation of CO over gold supported on TiO<sub>2</sub>, α-Fe<sub>2</sub>O<sub>3</sub>, and Co<sub>3</sub>O<sub>4</sub>. *J.Catal.* 144:175-192.
- Hu, L., Yang, X., Dang, S. (2011). An easily recyclable Co/SBA-15 catalyst: Heterogeneous activation of peroxydisulfate for the degradation of phenol in water. *Applied Catalysis B: Environmental.* 102:19-26
- Iizuka, Y., Miyamae, T., Miuraa, T., Okumura, M., Date, M., Haruta. M. (2009). A kinetic study on the low temperature oxidation of CO over Ag-contaminated Au fine powder. *J. Catal.* 262:280-286.
- Ingelsten, H., Zhao, D., Palmqvist, A., Skoglundh, M. (2005). Mechanistic study of the influence of

- surface acidity on lean NO<sub>2</sub> reduction by propane in HZSM-5 J. Catal. 232:68-79.
- Jiaqiao, L., Baiyun, H. (2001). Particle size characterization of ultrafine tungsten powder. Int. J. Refract Metals Hard Mat. 19:89-92.
- Kazuya, Y., Noritaka M. (2002). Supported ruthenium catalyst for the heterogeneous oxidation of alcohols with molecular oxygen. Angewandte Chemie International Edition, 41:4538-4542.
- Kohyama, M., Tomoki, A., Yasushi M. (2015). Low-temperature CO oxidation properties and TEM/STEM observation of Au/ $\gamma$ -Fe<sub>2</sub>O<sub>3</sub> catalysts. J. Catal. 324:127-132
- Kurzman J.A., Misch L.M., and Seshadri R. (2013). Chemistry of precious metal oxides relevant to heterogeneous catalysis. Dalton Trans. 42:146-153.
- Lin, S. D., Bollinger, M., Vannice, M. A. (1993). Low temperature CO oxidation over Au/TiO<sub>2</sub> and Au/SiO<sub>2</sub> catalysts. Catalysis Letters. 17: 245-262.
- Lindholm, A., Currier, N.W., Li, J., Yezerets, A., Olsson L. (2008). Detailed kinetic modeling of NO<sub>x</sub> storage and reduction with hydrogen as the reducing agent and in the presence of CO<sub>2</sub> and H<sub>2</sub>O over a Pt/Ba/Al catalyst J. Catal. 258:273-288.
- Liu, Q., Gao, J., Gu, F., Lu, X., Liu, Y., Li, H., Zhong, Z., Liu, B., Xu, G., Su, F. (2015). One-pot synthesis of ordered mesoporous Ni-V-Al catalysts for CO methanation. J. Catal. 326:127-138.
- Loneragan W. W., Wang, Vlachos, T., Chen. J. G. (2011). Effect of oxide support surface area on hydrogenation activity: Pt/Ni bimetallic catalysts supported on low and high surface area Al<sub>2</sub>O<sub>3</sub> and ZrO<sub>2</sub>. Applied Catal. 408:87-95.
- Mori, K., Hara, T., Mizugaki, T., Ebitani, K., Kaneda, K. (2004). Hydroxyapatite-supported palladium nanoclusters: a highly active heterogeneous catalyst for selective oxidation of alcohols by use of molecular oxygen. Journal of the American Chemical Society. 126:10657-10666.
- Ning, X., Yu, H., Peng, F., Wang, H. (2015). Pt nanoparticles interacting with graphitic nitrogen of N-doped carbon nanotubes: Effect of electronic properties on activity for aerobic oxidation of glycerol and electro-oxidation of CO. J. Catal. 325:136-144.
- NIST Standard Reference Database 69: NIST Chemistry WebBook.
- Nolan, M. (2013). Modifying ceria (111). with a TiO<sub>2</sub> nanocluster for enhanced reactivity. J. Chem. Phys. 139:18.
- Ohsaka, T., Izumi, F., Fujiki, Y. (1978). Raman spectrum of anatase, TiO<sub>2</sub>. J. Raman Spec. 7:321-324.
- Palcheva, R., Dimitrov, L., Tyuliev, G., Spojakina, A., Jiratova, K. (2013). TiO<sub>2</sub> nanotubes supported NiW hydrodesulphurization catalysts: Characterization and activity. Appl Surf Sci. 265:309-316,
- Park, K.W., Seol, K.S. (2007). Nb-TiO<sub>2</sub> supported Pt cathode catalyst for polymer electrolyte membrane fuel cells. Electrochemistry Communications. 9:2256-2260.
- Pérez, J., Kondratenko, E., Debbagh. M. (2005). Transient studies on the mechanism of N<sub>2</sub>O activation and reaction with CO and C<sub>3</sub>H<sub>8</sub> over Fe-silicalite. J. Catal. 233:442-452.
- Qu, Z., Zhang, X., Yu, F., Liu, X., Fu, Q. (2015). Role of the Al chemical environment in the formation of silver species and its CO oxidation activity. J. Catal. 321: 113-122.
- Ren, X. Zhang, H., Cui, Z. (2007). Acetylene decomposition to helical carbon nanofibers over supported copper catalysts. Materials Research Bulletin. 42:2202-2210.
- Rivallan, M., Ricchiardi, G., Bordiga, S., Zecchina, A. (2009). Adsorption and reactivity of nitrogen oxides (NO<sub>2</sub>, NO, N<sub>2</sub>O). on Fe-zeolites J. Catal. 264:104-116.
- Sheintuch, M., Schmidt, J., Lectham Y., Yahav, G. (1989). Modelling catalyst-support interactions in carbon monoxide oxidation catalysed by Pd/SnO<sub>2</sub>. Appl. Catal. 49:55-65.
- Tsao, C.S., Yu, M. S., Chung, T.Y., Wu, H. C., Yu Wang, C., Chang, K. S., Chen. H. L. (2007). Characterization of pore structure in metal-Organic framework by small-angle X-ray scattering J. Am. Chem. Soc. 129:15997-16004.
- Williamson, G.K., Hall, W.H. (1953). X-ray line broadening from filed aluminium and wolfram L'élargissement des raies de rayons x obtenues des limailles d'aluminium et de tungstène Die verbreiterung der roentgeninterferenzlinien von aluminium- und wolframspaenen Acta Metall. 1:22-31.
- Wonyong, C., Sang-Hyup, L., Palanichamy, M., Narayanan, L., Jae, Y., Jae, S., Jonghun. L. (2014). Synergic photocatalytic effects of nitrogen and niobium co-doping in TiO<sub>2</sub> for the redox conversion of aquatic pollutants under visible light J. Catal. 310:91-99.
- www.micromeritics.com. Gas Adsorption Theory.
- Xianyong S, S., Mueller, S., Shi, H., Haller, G., Sanchez-Sanchez, M., A. Van Veen, J. Lercher. (2014). On the impact of co-feeding aromatics and

olefins for the methanol-to-olefins reaction on HZSM-5 J. Catal. 314:21-31.

Yan, W., Mahurin, S. M., Pan, Z., Overbury, S. H., Dai, S. (2005). Ultrastable Au nanocatalyst supported on surface-modified TiO<sub>2</sub> nanocrystals. Journal of the American Chemical Society. 127:10480-10481.

Yasuo, I., Tomonobu, M., Takumi, M., Mitsutaka, O., Masakazu, D., Masatake, H. (2009). A kinetic study on the low temperature oxidation of CO

over Ag-contaminated Au fine powder J. Catal. 262:280-286.

Young, Y., Meijun, L., Wolfgang, M.S., Weitz, E. (2007). Low-temperature NO<sub>x</sub> reduction with ethanol over Ag/Y: A comparison with Ag/ $\gamma$ -Al<sub>2</sub>O<sub>3</sub> and BaNa/Y. J. Catal. 246:413-427.

Zhao, Z., Li, Z., Lin, Y. S. (2009). Adsorption and diffusion of carbon dioxide on metal-organic framework (MOF-5). Ind. Eng. Chem. Res. 48:10015-10020.